Applied Catalysis B: Environmental 179 (2015) 589–598

Contents lists available at ScienceDirect

Applied Catalysis B: Environmental

journal homepage: www.elsevier.com/locate/apcatb

IR studies of Fe modified ZSM-5 zeolites of diverse mesopore topologies in the terms of their catalytic performance in NH_3-SCR and NH_3-SCO processes

Kinga Góra-Marek[a,*], Kamila Brylewska[b], Karolina A. Tarach[a], Małgorzata Rutkowska[a], Magdalena Jabłońska[a], Minkee Choi[c], Lucjan Chmielarz[a]

[a] Faculty of Chemistry, Jagiellonian University in Kraków, 3 Ingarden Street, 30-060 Kraków, Poland
[b] Faculty of Materials Science and Ceramics, AGH University of Science and Technology in Kraków, 30 Mickiewicz Av., 30-059 Kraków, Poland
[c] Department of Chemical and Biomolecular Engineering, Korea Advanced Institute of Science and Technology, Republic of Korea

ARTICLE INFO

Article history:
Received 22 March 2015
Received in revised form 25 May 2015
Accepted 29 May 2015
Available online 1 June 2015

Keywords:
Fe-zeolites
ZSM-5
NH_3-SCR and NH_3-SCO
NO sorption
IR spectroscopy

ABSTRACT

The desilication and direct synthesis route techniques were used to prepare mesostructured ZSM-5 zeolites. Iron was introduced to purely microporous and to hierarchical analogs by two-fold ion-exchange procedure using a $Fe(NO_3)_3$ solution. The results of the catalytic studies of the NH_3-SCR process showed that the Fe-exchanged ZSM-5 sample prepared by direct synthesis route with amphiphilic organosilanes as a mesopore-directing agents presented the highest catalytic activity in the low temperature range comparing to the other catalyst studied. Moreover, the Fe-catalysts revealed high catalytic performance in the NH_3-SCO process. High catalytic activity of the studied samples was related to high concentration of mononuclear Fe^{3+} cations with pseudo-T_d or O_h coordination, guaranteed by the enhanced mesopore area of zeolite support, as well as with high acidity of the zeolite itself. The facility of the transport of the reactants to and from the active surface sites seems to be also ensured by highly developed system of mesopores. IR studies of adsorption forms both of nitrogen monoxide and ammonia as well as the products of their conversion gave insight into the NH_3-SCR and NH_3-SCO reaction mechanisms.

1. Introduction

The selective catalytic reduction of NO_x with ammonia (NH_3-SCR, $DeNO_x$) is the most important and well-established process used to abate nitrogen oxides ($NO_x = NO + NO_2$) from stationary and mobile sources [e.g.,1,2]. In a typical NH_3-SCR process, the ratio of NO to NH_3 is 1:1 (Eq. (1)).

$$4NO + 4NH_3 + O_2 = 4N_2 + 6H_2O \quad (1)$$

One of the main drawbacks related to the NH_3-SCR applications is a risk of ammonia slip referring to the emission of unreacted ammonia that result from uncompleted Reaction (1). To avoid ammonia slip, NH_3-SCR is performed under stoichiometric amount of ammonia resulting in a reduced efficiency of NO_x elimination. However the abatement of NO_x emissions can be realized with stoichiometric and even an excess quantity of NH_3 when the catalysts for the oxidation of residual ammonia into nitrogen and water vapor are employed. Finally, the selective catalytic oxidation of ammonia into dinitrogen and water vapor (NH_3-SCO) is the most promising technology of ammonia conversion in oxygen-containing waste gases especially when the same catalyst guarantees high activity in both the NH_3-SCO and NH_3-SCR processes. It has been recognized that the conversion of NO via NH_3-SCR takes place at lower temperatures than a conversion of ammonia via NH_3-SCO.

A large number of reports providing promising catalytic performance of various Fe-based materials, including ion-exchanged ZSM-5, in NH_3-SCR and/or NH_3-SCO was presented in the scientific literature [e.g.,3–8 and references therein]. The substantial effort has been paid to analyze the nature and the role of the respective Fe species in those reaction mechanisms. The influence of both type of support and the Fe-precursors as well as the method Fe-deposition were subjected to detailed investigation. Qi et al. [3,4] investigated effect of iron deposition into ZSM-5 on its catalytic performance in both the NH_3-SCR and NH_3-SCO processes. In NH_3-SCO reaction Fe-ZSM-5 prepared by sublimation of $FeCl_3$ showed over 99% NH_3 conversion and nearly 100% selectivity to N_2 at 400 °C [4]. Additionally, such catalyst was found to be the most active among different

* Corresponding author. Tel.: +48 12 663 20 81; fax: +48 12 6340515.
E-mail address: kinga.goramarek@gmail.com (K. Góra-Marek).

http://dx.doi.org/10.1016/j.apcatb.2015.05.053
0926-3373/

Fe-zeolite catalysts prepared by sublimation method at 700 °C with following order: Fe-ZSM-5 > Fe-MOR > Fe-FER > Fe-Beta > Fe-Y > Fe-ASA (amorphous silica alumina) [3,8]. The studies of application of various iron precursors (e.g., $FeCl_3$, $FeCl_2$ and $FeSO_4$) deposition on ZSM-5 by impregnation method were also reported. The $FeCl_3$ was found to be the most suitable for iron deposition than other iron salts, nevertheless all the studied catalysts revealed over 95% NH_3 conversion with around 99% selectivity to N_2 at 500 °C [3]. Also the Fe-exchanged ZSM-5, prepared using $FeCl_2$, was proved to be superior to other supported transition/noble metals both in NH_3-SCR and NH_3-SCO processes [7]. The difference in activity was correlated with the ability of Fe-ZSM-5 to form stabilized binuclear Fe(III) complexes, which are the active sites in the NH_3-SCO process [9]. Additionally, it was suggested that isolated pseudotetharedral Fe(III) species, present in different types of zeolites containing iron including Fe-ZSM-5, are responsible for their high catalytic performances in the NH_3-SCR process [10,11].

Mesoporous Fe-ZSM-5 zeolites were reported to present the improved catalytic properties compared to conventional microporous zeolitic materials both in NH_3-SCR and NH_3-SCO [e.g.,12,13]. The samples containing 6–7 wt.% of Fe deposited by impregnation method, using a $Fe(NO_3)_3$ solution, revealed high catalytic activity. It was possible to achieved 100% NO conversion at 450 °C in the presence of this catalyst [12,13]. However, no clarification in the speciation of iron species and aggregation neither state nor reaction mechanism over tested materials were presented. Additionally, it seems that there are not any reports in the scientific literature presenting the studies of selective catalytic oxidation of ammonia over mesoporous zeolites. The objective of this paper is to fill this gap.

Our studies are focused on modification methods, such as desilication and direct synthesis route, in order to create mesoporosity in commercial ZSM-5 zeolites. Direct synthesis route with amphiphilic organosilanes allow for obtaining the nanocrystalline zeolitic material with the 10 nm average size of grains [13]. Iron was deposited using the two-fold ion-exchange procedure. The purely microporous zeolite Fe-ZSM-5 was used as the reference catalyst. All the samples were characterized with respect to their physicochemical properties and their catalytic performances in selective catalytic reduction of NO with ammonia and selective catalytic oxidation of ammonia into dinitrogen and water vapour. Another scope was the studies of the reaction mechanisms for both the NH_3-SCR and NH_3-SCO processes.

2. Experimental methods

2.1. Catalyst preparation

Parent ZSM-5 of Si/Al = 32, hereafter denoted as ZSM-5/P, was purchased from Zeolyst Company (CBV 5524G). Zeolite ZSM-5/D was obtained from ZSM-5/P by alkaline leaching in a 0.2 M NaOH + TBAOH (TBAOH: tetrabuthylammonium hydroxide) solution at 80 °C for 5 h. After desilication, the suspension was cooled down in ice-bath, filtered, and washed with distillate water until neutral pH. Next fourfold Na^+/NH_4^+ ion-exchange with 0.5 M NH_4NO_3 was performed at 60 °C for 1 h. Finally, the resulting sample was again filtrated, washed, and dried at room temperature.

Zeolite HZSM-5/M of tuneable mesoporosity was obtained via a direct synthesis route using the amphiphilic organosilanes as a mesopore-directing agent according to procedure presented in Ref. [14].

Zeolites of various pore topology were subjected to two-fold ion-exchange procedure with a 0.05 M $Fe(NO_3)_3$ solution (1 g of zeolite per 100 ml of solution) that was performed at 60 °C for 1 h. Finally, the resulting Fe-sample was again filtrated, washed, and dried at room temperature. The notation applied for native Na or H- zeolites was preserved for their Fe-analogs.

2.2. Characterization techniques

2.2.1. Chemical analysis of metal content, structural and textural studies

DR UV–vis spectroscopy was applied to determine the chemical nature of iron species dispersed in zeolites of various pore hierarchy. DR UV–vis spectra were acquired on a Cary 5000 Varian spectrometer equipped with a double integrator with polytetrafluoroethylene as a reference. The measurements were performed in the range of 200–600 nm with a resolution of 2 nm.

The powder X-ray diffraction (XRD) measurements were carried out using a X'Pert Pro Philips (PANalytical Cubix diffractometer), with CuKα radiation, λ = 1.5406 Å and a graphite monochromator in the 2θ angle range of 5–40°. X-ray powder patterns were used for structural identification of the relative crystallinity value (%Cryst) for all the zeolites. Determination of the relative crystallinity was based on the intensity of the reflections in the range between 10 and 60°.

The content of Fe, Si and Al in studied materials were determined by the XRF method using an Energy-Dispersive XRF spectrometer (Thermo Scientific, ARL QUANT'X with the Rh anode, the X-rays of 4–50 kV (1 kV step), 1 mm size beam). A 3.5 mm Si(Li) drifted crystal with a Peltier cooling (∼ − 88 °C) was used as a detector.

The textural parameters of the samples were determined by N_2 sorption at −196 °C using a 3Flex v.1.00 (Micromeritics) automated gas adsorption system. Prior to the analysis, the samples were degassed under vacuum at 250 °C for 24 h. The specific surface area (S_{BET}) was determined using BET (Braunauer–Emmett–Teller) model according to Rouquerol recommendations [15]. The micropore volume (at $p/p_0 = 0.99$) and specific surface area of micropores were calculated using the Harkins and Jura model (*t*-plot analysis).

2.2.2. IR spectroscopy studies with probe molecules

Prior to FTIR studies, all studied zeolites were pressed into the form of self-supporting wafers (ca. 5–10 mg/cm^2) and pre-treated in situ in an IR cell at 500 °C under vacuum conditions for 1 h. Spectra were recorded with a Bruker Tensor 27 spectrometer equipped with a MCT detector with the spectral resolution of 2 cm^{-1}. All the spectra presented in this work were normalized to 10 mg of the sample.

Total concentration of the Brønsted and Lewis acid sites in calibration materials was determined in quantitative IR studies of ammonia sorption (PRAXAIR, ≥99.8%). The excess of ammonia was adsorbed at 100 °C, and then physisorbed molecules were removed by the evacuation at the same temperature. For quantitative consideration on the number of catalytically active sites the intensities of the bands of ammonia coordinatively bonded to Lewis acid sites (NH_3L) and to Brønsted one (NH_4^+) were taken, by applying the respective extinction coefficients: 0.11 cm^2 μmol^{-1} for the NH_4^+ band and 0.026 cm^2 μmol^{-1} for the NH_3L band.

With regard to the NH_3-SCR process elucidation the sorption of nitrogen monoxide (Linde Gas Poland 99.5%) was performed on the vacuum treated samples as well as on materials saturated with ammonia. In all cases NO was sorbed at 100 °C, then the temperature of the system was gradually increased to 200 °C. After contact time of 10 min. the IR cell was cooled down to room temperature and IR spectrum was collected.

The NH_3-SCO reaction was followed in the ammonia and oxygen sorption experiments. The excess of ammonia was adsorbed at 100 °C, and then physisorbed molecules were removed by the evacuation at the same temperature. Next, the sample with preadsorbed ammonia was contacted with oxygen (Linde Gas Poland

Table 1
Chemical analysis results of native zeolites and their Fe-forms.

Zeolite code	Si/Al	Al_{XRF} [μmol/g]	Al_{XRF} [−/u.c.]	Fe/Al	Fe_{XRF} [μmol/g]	Fe_{XRF} [−/u.c.]
ZSM-5/P	32	472	2.91	0	0	0
Fe-P				0.20	94	0.58
ZSM-5/D	21	698	4.36	0	0	0
Fe-D				0.16	103	0.65
ZSM-5/M	27	549	3.43	0	0	0
Fe-M				0.25	143	0.88

99.9%) (NH_3:O_2 = 1:5) and the reaction was tracked by the IR spectra collecting at increasing temperature (up to 350 °C).

2.3. Catalytic tests

Catalytic studies of selective reduction of NO with ammonia (NH_3-SCR) and selective oxidation of ammonia (NH_3-SCO) were performed in a fixed-bed flow microreactor system. The experiments were carried out under atmospheric pressure and in the temperature range from 70 to 500 °C. For each experiment 0.1 g of catalyst (particles sizes in the range of 0.160–0.315 mm) was placed on quartz wool plug in the quartz tubular reactor and outgassed in a flow of pure helium at 500 °C for 1 h. The gas mixture containing for: (i) NH_3-SCR reaction: 0.25–vol.% of NO, 0.25–vol.% of NH_3 and 2.5–vol.% of O_2 and (ii) NH_3-SCO reaction: 0.5–vol.% of NH_3 and 2.5–vol.% of O_2, diluted in pure helium (total flow rate of 40 ml/min) was used.

A quadrupole mass spectrometer RGA 100 (PREVAC) connected directly to the reactor outlet was used for analysis of reactants (NH_3, NO, O_2) as well as all possible reaction products (N_2, NO, N_2O, NO_2, H_2O). The NO conversion (α_{NO}) in the NH_3-SCR process was determined using the following equation:

$$\alpha_{NO} = \frac{C_{0NO} - C_{NO}}{C_{0NO}} \times 100\%$$

where: C_{0NO} – concentration of NO in inlet gases; C_{NO} – concentration of NO in outlet gases.

Apart from N_2 and N_2O any other nitrogen-containing products of the NH_3-SCR process were detected, therefore the selectivity toward nitrogen was calculated according to the following equation.

$$S_{N_2} = \frac{C_{N_2}}{C_{N_2} + C_{N_2O}} \times 100\%$$

where: C_{N_2} and C_{N_2O} – concentrations in outlet gases of N_2 and N_2O, respectively.

The NH_3 conversion (α_{NH3}) in the NH_3-SCO process was determined using the following equation:

$$\alpha_{NH_3} = \frac{C_{0NH_3} - C_{NH_3}}{C_{0NH_3}} \times 100\%$$

where: C_{0NH_3} – concentration of NH_3 in inlet gases; C_{NH_3} – concentration of NH_3 in outlet gases.

In the NH_3-SCO process, among nitrogen-containing products only N_2, N_2O and NO were detected. Therefore, for calculation of the process selectivity to N_2 the following equation was used:

$$S_{N_2} = \frac{C_{N_2}}{C_{N_2} + C_{N_2O} + \frac{1}{2}C_{NO}} \times 100\%$$

where: C_{N_2}, C_{N_2O} and C_{NO} – concentrations in outlet gases of N_2, N_2O and NO, respectively.

The selectivities to NO and N_2O were calculated using analogous equations.

The space time (τ) of NO in these conditions, defined as $\tau = W/\dot{n}_{NO}$ (where: W is a catalyst mass, and $\dot{n}_{NO}$ is a molar flow of NO in the inlet mixture) was equal to 373 g h mol^{-1}. By analogy, the space time of NH_3 in used conditions was equal to 187 g h mol^{-1}.

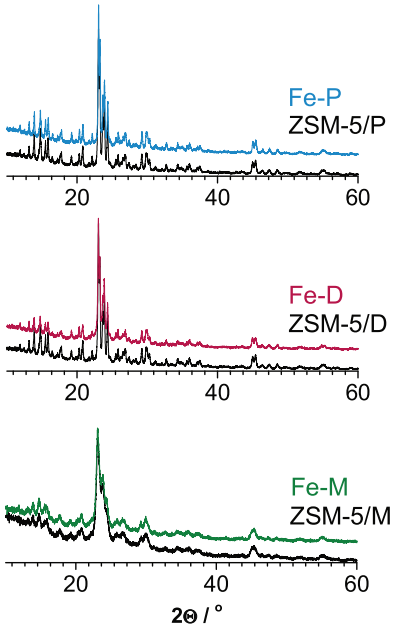

Fig. 1. XRD patterns of H- and Fe-zeolites.

To elucidate the influence of the iron speciation on catalytic performance, the catalysts previously H_2-reduced at 500 °C for 15 min. were tested in NH_3-SCR and NH_3-SCO. Detailed information on the speciation of Fe-sites in reduced zeolite materials in included in Ref. [16].

3. Results

3.1. Physicochemical characterization of the catalysts

Iron modified zeolitic materials of different origin of mesoporous system generation were characterized with regard to their structural and textural properties as well as to the speciation of catalytically active metal component. Results of chemical analysis of the native zeolites and their Fe-forms are gathered in Table 1.

XRD patterns recorded for all mesoporous zeolites (ZSM-5/M and ZSM-5/D) are typical of the ZSM-5 structure (Fig. 1). The crystallinity (%Cryst., Table 2) was preserved for both hierarchical zeolites, however, a lowered crystallinity of Fe-M zeolite was evidenced. Additionally, the line broadening in the XRD peaks can suggest that the mesoporous zeolite particles were built with randomly oriented zeolite nanocrystals. The results of XRD studies of native and Fe-modified zeolites confirmed the stability of all the zeolite structures against the impregnation and/or calcination procedure (Fig. 1). Independently from the Fe-loading (1.0–1.5 wt.%) and type of generated mesoporosity any reflections characteristic of Fe(II) or Fe(III) oxide species were not recognized in diffractograms of Fe-modified zeolites. The formation of highly dispersed,

Table 2
Textural parameters of native zeolites and their Fe-forms.

Zeolite code	%Cryst	S_{total} [$m^2 g^{-1}$]	S_{meso} [$m^2 g^{-1}$]	V_{micro} [$cm^3 g^{-1}$]	V_{meso} [$cm^3 g^{-1}$]
ZSM-5/P	100	377	40	0.17	0.06
Fe-P		360	35	0.15	0.05
ZSM-5/D	89	308	145	0.15	0.21
Fe-D		300	143	0.13	0.20
ZSM-5/M	82	520	187	0.16	0.35
FeM-2		480	188	0.12	0.33

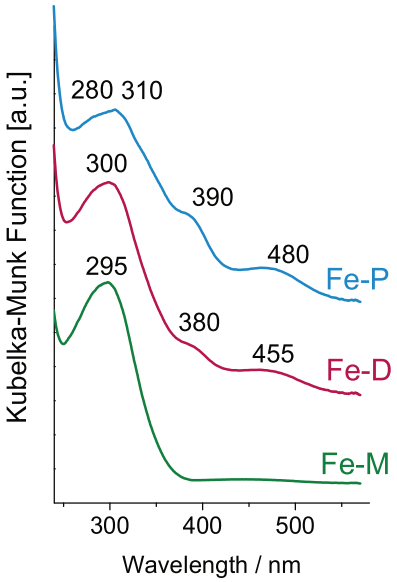

Fig. 2. DR UV–vis spectra of the Fe-exchanged zeolites ZSM-5.

thus an amorphous nature Fe-moieties, was suggested for all the zeolitic matrixes. The existence of oxide-like species, which growing was restricted by the pore size of zeolite ZSM-5 and therefore not sufficient in particle size to be discriminated from the zeolite pattern was widely discussed [2,7].

Highly developed BET surface areas for hierarchical zeolites ZSM-5/D and ZSM-5/M evidenced development of mesoporosity with preservation of their microporous character (Table 2). The influence of the Fe-species presence on the textural parameters of the catalysts was also examined (Table 2). It was recognized that introduction of Fe species to ZSM-5 zeolites only slightly affected their textural parameters. Only small decrease in micropore volume clearly evidenced the partial plaguing of the micropore system due to accommodation of Fe-species.

3.2. DR UV–vis spectroscopy studies

DR UV–vis spectroscopy was applied to recognize the coordination and aggregation of Fe species dispersed in zeolites of various pore hierarchy.

Fig. 2 presents the DR UV–vis spectra of purely microporous zeolite ZSM-5 and its hierarchical analogs modified with Fe. The samples exhibit strong absorption bands in the range of 250–550 nm. The monomeric Fe^{3+} ions in tetrahedral coordination are characterized by the absorption bands located below 250 nm. The bands at ca. 295–310 nm observed in DR UV–vis spectrum of FeZSM-5 zeolites are attributed to pseudotetrahedral or octahedral Fe^{3+} located in $Fe(III)O^+$, dinuclear $[Fe(III)–\mu O_2–Fe(III)]^{2+}$ species or defined polynuclear Fe(III)-oxo complexes [17–20]. The absorption region corresponding to less dispersed oligomeric Fe_xO_y species is located in the range of 300–400 nm, while Fe_2O_3 nanoparticles are identified by the bands above 400 nm [18,20]. Iron introduced to the purely microporous zeolite (Fe-P) bears four possible forms (mononuclear cations with T_d and O_h coordination, oligomeric iron oxide clusters and Fe_2O_3 species). In contrast, well dispersed Fe^{3+} cations either in the form of mononuclear Fe^{3+} cations with pseudo-T_d or O_h coordination as well as oligonuclear clusters are the dominant iron forms introduced into all zeolitic matrixes independently from the porosity character. The presence of oligomeric iron oxide clusters and Fe_2O_3 species is noticeably high only in Fe-P zeolite. No band characteristic for Fe_2O_3 nanoparticles was detected in zeolite obtained by amphiphilic organosilanes route thus the uniform micro/mesoporous structure of Fe-M is believed to prevent clustering of iron moieties and preserves the Fe(III) isolated and/or dinuclear species with pseudo-T_d or O_h coordination inside zeolite channels.

3.3. Catalytic tests

3.3.1. NH_3-SCR performance

The obtained samples were tested as catalysts in the process of selective catalytic reduction of NO with ammonia (1) as well as selective catalytic oxidation of ammonia to dinitrogen (2):

$$4NH_3 + + 4NO + O_2 \rightarrow 4N_2 + 6H_2O \quad (1)$$

$$4NH_3 + 3O_2 \rightarrow 2N_2 + 6H_2O \quad (2)$$

The results of the NH_3-SCR tests are presented in Fig. 3. Additionally, the results of the catalytic tests were summarized in Table 3, which presents the highest conversion of nitrogen monoxide as well as selectivity to N_2 at the same temperatures. The reference ZSM-5/P sample without iron was not catalytically active in the NO conversion in the entire temperature range. Modification of zeolites with iron significantly activated them in the NH_3-SCR process. The NO conversion starts at about 150 °C and slowly increases to 225 °C reaching the level of 14% in the presence of conventional ZSM-5 zeolite doped with iron (Fe-P). At higher temperatures the NO conversion slightly decreases and then, starting from 275 °C sharply increases reaching 95% at 500 °C. The catalysts based on zeolites with the hierarchical porous structure effectively activate the NH_3-SCR process in the low temperature range. In this case NO was converted to dinitrogen at temperature as low as 100 °C and efficiency of this process sharply increases to 375 °C reaching the level of NO conversion nearly 100%. The ammonia conversions profiles are very similar to the profiles of NO conversion in the low- temperature range indicating that $DeNO_x$ reaction dominates under these conditions, while the differences in profiles of NO and NH_3 conversions at higher temperatures are related to direct oxidation of ammonia by oxygen present in the reaction mixture mainly to nitrogen. In a group of the catalysts based on zeolites with the hierarchical porous structure the best results, with respect to high activity and selectivity to N_2 (97–100%), were obtained for hierarchical zeolite Fe-M. The sample Fe-D was less active and selective. It is also worth to mention that the selectivity to N_2, in case of all the samples, is very high and does not drop below 90% in the entire temperature range. The reaction temperature increase above 375 °C results in a dramatic decrease in efficiency of the NO conversion. This effect is related to the inten-

Table 3
Summary of the results of catalytic tests.

Zeolite code	NH_3-SCR		NH_3-SCO	
	Conversion/% (temperature/°C)	N_2 selectivity/%	Conversion/% (temperature/°C)	N_2 selectivity/%
ZSM-5/P	–	–	65 (500)	85
Fe-P	97 (500)	100	88 (500)	97
Fe-D	93 (375)	94	94 (500)	95
Fe-M	100 (375)	98	99 (500)	98
Fe-P/R	97 (500)	79	75 (500)	93
Fe-D/R	82 (375)	77	91 (500)	90
Fe-M/R	95 (375)	90	99 (500)	87

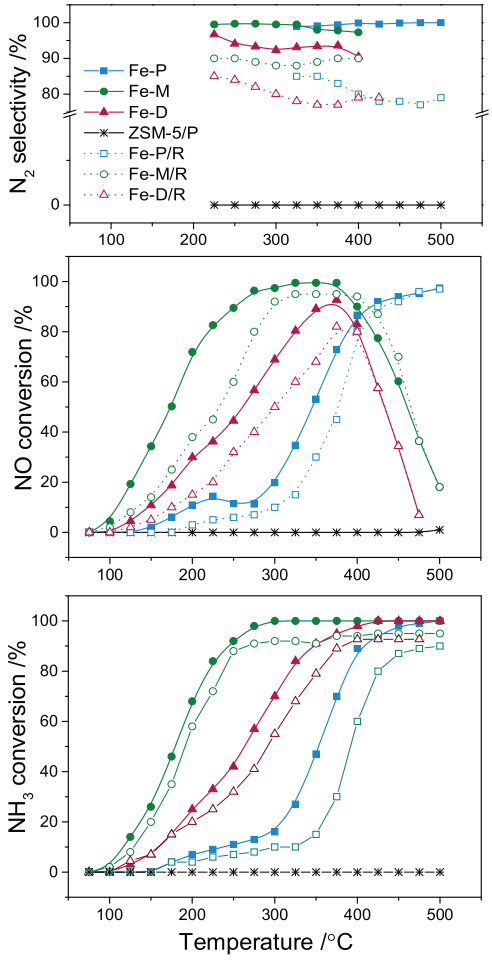

Fig. 3. Results of catalytic tests for the NH_3-SCR process performed for Fe-P (squares), Fe-M (circles), Fe-D (tringles) and HZSM-5 (stars). Reaction conditions: 0.25 vol.% of NO, 0.25 vol.% of NH_3 and 2.5 vol.% of O_2; He as balancing gas; total flow rate – 40 ml/min; weight of catalyst – 0.1 g. Solid symbols: the catalysts outgassed in a flow of pure helium at 500 °C for 1 h; empty symbols: the catalysts previously H_2-reduced at 500 °C for 15 min.

sive side-process of direct ammonia oxidation by oxygen present in the reaction mixture. Pretreatment of the catalysts in reducing atmosphere before catalytic tests resulted in their lower activity and selectivity. For the reduced Fe-P sample, the NO conversion starts at temperatures higher by about 50 °C compared to the non-reduced sample. However, the NO conversion of 97% at 500 °C was obtained for both the Fe-P and Fe-P/R catalysts. The NO conversion for Fe-M/R and Fe-D/R maintained the highest level at 375 °C, however, lower catalytic activity was found for these samples compared to the non-reduced catalysts (see Table 3). Comparison of the results of catalytic studies performed in various laboratories is always speculative mainly due to various conditions used in these catalytic tests. However, sometimes such comparison is necessary to evaluate the relative efficiency of the obtained catalytic systems. There is a lot of studies presenting application of ZSM-5 modified with iron in the role of the NH_3-SCR catalysts. Brandenberger et al. [21] reported studies of ZSM-5 modified with iron by ion exchange method in the role of catalysts for NH_3-SCR. For the most active catalysts included in these studies 90% of NO conversion was obtained at about 350 °C, so at temperature higher by about 100 °C in comparison to presented in this work the ZSM-5 with tuneable mesoporosity modified with iron (Fe-M). Also results presented by Shi et al. [22] for ZSM-5 modified with iron by ion-exchange method and Santhosh Kumar et al. [23] for ZSM-5 doped with iron by chemical vapor deposition, solid state ion-exchange and mechano-chemical route showed lower efficiency in the NO conversion comparing to the results obtained for the Fe-M catalysts. However, it must be underlined that the mentioned above studies were performed in different conditions (higher GHSV and lower content of NO and NH_3 comparing to the experiments presented in this paper), and therefore, such comparison should be treated only as a rough evaluation of the activity of the studied samples. The presented above comparison led to the conclusion that non-reduced zeolites with the hierarchical porous structure and iron oxide species (Fe-M) can be confidently assigned to the group of promising catalysts for the low-temperature NH_3-SCR process. Further elaboration of literature sources also confirm those conclusions, as the obtained results confirm very high selectivity to N_2 (97–100%) of studied zeolites (see Supplementary information and references therein).

3.3.2. NH_3-SCO performance

The relationship between NH_3-SCR and NH_3-SCO reactions has been widely discussed. E.g., Qi et al. [3,4] tested Fe-exchanged zeolites and found that higher activity in NH_3-SCR reaction reflected higher selectivity to N_2 in the NH_3-SCO process. These findings, together with above presented results of catalytic tests for the NH_3-SCR process, were inspiration for testing of modified zeolites as potential catalysts for selective oxidation of ammonia to dinitrogen. The catalysts of the NH_3-SCO process should operate in a relatively low-temperature range that reduces costs of additional heating of waste gases and should selectively convert ammonia to dinitrogen.

The results of selective catalytic oxidation of ammonia over the zeolite based catalysts are shown in Fig. 4, while temperature of maximum ammonia conversion as well as selectivity to N_2 at these temperatures are compared in Table 3. For the reference ZSM-5/P sample ammonia oxidation starts at temperatures as high as 375 °C and at 500 °C reached 65% with 85% selectivity to N_2. The ammonia oxidation for all the iron modified samples starts at about 250 °C, however, in case of the catalysts with the hierarchical porous structure ammonia conversion increases much faster with raising the reaction temperature in comparison to purely microporous Fe-P. Thus, the generation of mesoporosity in ZSM-5 has a strong impact on the catalytic activity in the NH_3-SCO process. Selectivity is a very important issue of this process. Dinitrogen, which is a

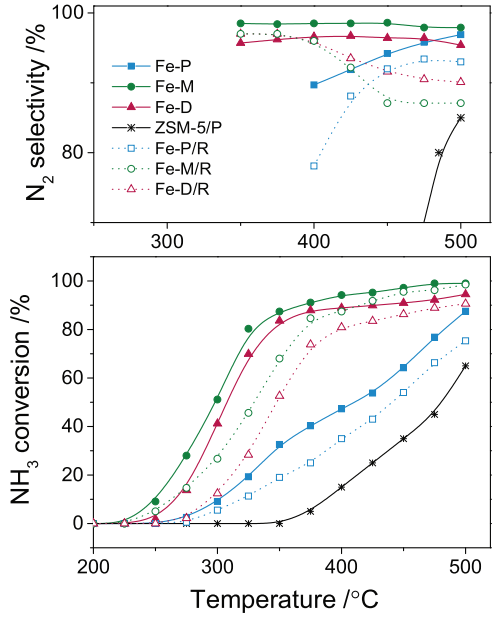

Fig. 4. Results of catalytic tests for the NH_3-SCO process performed for Fe-P (squares), Fe-M (circles) Fe-D (tringles) and HZSM-5 (stars). Reaction conditions: 0.5 vol.% of NH_3 and 2.5 vol.% of O_2; He as balancing gas; total flow rate – 40 ml/min; weight of catalyst – 0.1 g. Solid symbols: the catalysts outgassed in a flow of pure helium at 500 °C for 1 h; empty symbols: the catalysts previously H_2-reduced at 500 °C for 15 min.

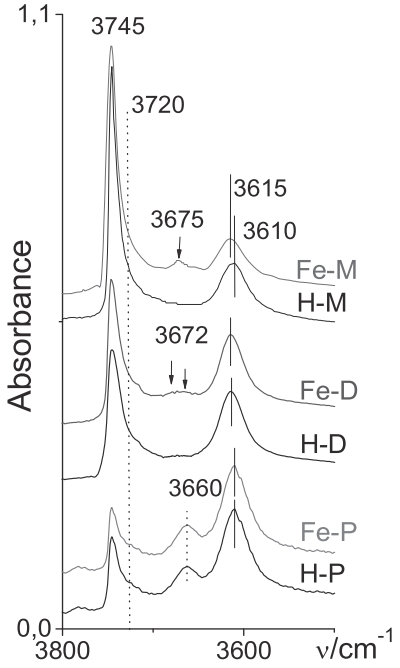

Fig. 5. IR spectra of H- and Fe-form of studied zeolites in the region of O—H stretching vibration.

desired reaction product, was the main product of ammonia oxidation, formed with the selectivity above 90% at temperature as high as 475 °C. All reduced catalysts revealed lower catalytic activity than the non-reduced samples. This effect was significantly higher for mesostructured zeolites Fe-M/R and Fe-D/R than for microporous Fe-P/R, especially at temperatures below 400 °C. In contrast, selectivity to N_2 decreased for both the Fe-M/R and Fe-D/R samples above this temperature and finally reached 87–90% at 500 °C. Such effect was not found for the Fe-P/R sample, however H_2-pretreatment resulted in a decrease of its catalytic performance (see Table 3). Concluding, non-reduced iron modified zeolites with the hierarchical porous structure are very interesting catalysts for selective oxidation of ammonia, operating in a relatively broad temperature range including also high temperatures.

3.4. IR spectroscopy studies

3.4.1. Nature of hydroxyl group

IR spectra of H- and Fe-zeolites in the region of stretching O—H vibration are presented in Fig. 5. The acidic bridging Si(OH)Al groups are characterized by the 3610 cm^{-1} band. Additionally, silanol group Si—OH in defects (the 3720 cm^{-1} band) and Si—OH on external surfaces and mesopore surfaces (the 3745 cm^{-1}) can be distinguished. The fabrication of mesopore system is usually detected as a distinct increase of the silanols amount on mesopore surfaces. In the spectra of microporous H—P a band at 3660 cm^{-1} is also discernible being ascribed to OH groups associated with extraframework aluminum species [24]. The main characteristic of Fe-exchanged zeolites is a decrease of the intensity of the bridging Si(OH)Al groups which is attributed to the substitution of protons for positively charged Fe(III) species. The reduction of the intensity of 3610 cm^{-1} band is negligible for Fe-P suggesting the presence of less dispersed iron oxide species, that possessing their own anions, are not involved into neutralization of zeolite framework. The extent of the elimination of Si(OH)Al groups is the most pronounced for hierarchical Fe-M zeolite. Consequently, Fe-M zeolite accommodates the highest amount of the exchangeable positively charged iron cationic species.

Table 4
Concentrations (in μmol g^{-1}) of iron determined by XRF analysis. The Brønsted (B) and Lewis (L) acid sites determined in quantitative IR studies of ammonia sorption in studied zeolites. Fe_{IR} represents the concentration of Lewis sites assigned to Fe-species.

Zeolite code	Fe_{XRF} μmol g^{-1}	B μmol g^{-1}	L μmol g^{-1}	Fe_{IR} μmol g^{-1}
ZSM-5/P	0	390	30	
Fe-P	94	410	34	4
ZSM-5/D	0	621	105	
Fe-D	104	500	145	40
ZSM-5/M	0	342	100	
Fe-M	143	270	175	75

The most catalytically active iron species in Fe-exchanged zeolites FER, BEA, and MFI are associated with highly reactive and weakly acidic isolated Fe^{3+}-OH hydroxyls represented by IR band at 3670–3680 cm^{-1} [25–28]. The Fe^{3+}-OH sites were reported to be easily reduced by NO to Fe^{2+} species even at low temperatures producing nitrate species. On the other hand, thermal decomposition of nitrates led to restoration of the Fe^{3+}-OH groups [29]. The Fe^{3+}-OH band decreased during H_2-treatment, and was restored when the reduced sample was oxidized by O_2 or N_2O [28]. The scrutiny of the IR spectra of studied Fe-exchanged zeolites also revealed the presence of the 3675 cm^{-1} Fe^{3+}-OH band. The Fe^{3+}-OH sites hosted in studied Fe-zeolites points to their potential catalytic activity in NH_3-SCR and NH_3-SCO reactions.

3.4.2. Quantification of acid sites with ammonia

Ammonia molecule is probe molecule used for quantification of both Brønsted and Lewis sites in solid acid catalysts [30]. Interaction of ammonia with Brønsted and Lewis acid sites results in the development of the 1465–1450 cm^{-1} and 1625–1600 cm^{-1} band, respectively. In present work, the concentrations of both Brønsted (NH_4^+) and Lewis (NH_3L) acid sites were calculated on the bases of the maximum intensities of the NH_4^+ and NH_3L bands as well as corresponding values of the extinction coefficients, which were determine as described in Refs. [31,32]. Table 4 gathers the

concentrations of Brønsted and Lewis acid sites determined in IR quantitative measurements of ammonia sorption in both Fe-modified zeolites ZSM-5 and their native forms. The difference in the concentrations of Lewis centers in Fe- and H-zeolites is related to the various amounts of Fe centers able to bond ammonia molecules. Neither the concentrations of Brønsted nor Lewis sites were influenced by Fe introduced to zeolite Fe-P indicating the presence of highly agglomerated Fe-oxide forms that not deliver Lewis acidity. Also DR UV–vis spectroscopy confirmed noticeable amounts of oligomeric iron oxide clusters and Fe_2O_3 in Fe-P. On the other hand, in comparison to H-forms of studied ZSM-5 zeolites, Fe-modified mesostructured zeolites were characterized by the lower Brønsted and enhanced Lewis acid sites amounts. Nevertheless, only for zeolite Fe-M the drop of Brønsted acidity was reflected in the formation of the equivalent quantity of Lewis acid sites. Therefore, the isolated pseudotetrahedral Fe^{3+} sites are supposed to occupy the extraframework positions in zeolite Fe-M, in line with both IR and DR UV–vis results. The concentration of Lewis sites found in Fe-exchanged desilicated zeolite Fe-D corresponded to 30% of the Brønsted sites consumed due to ion-exchange procedure. Consequently, the presence of pseudotetrahedral Fe^{3+} sites and polinuclear/agglomerated oxide forms cannot be excluded in case of zeolite Fe-D.

The surface acidity of the catalyst is a vital factor affecting the activity in selective ammonia oxidation into nitrogen and water vapor. The presence of surface acid sites of high strength influences the capturing of ammonia nearly the active TMI moieties. The ammonia bonded coordinatively to Lewis acid sites and/or existing in the form of ammonium ions (due to reaction with Brønsted acid sites) can be considered as additional reservoir of ammonia chemisorbed. Thus, the TMI-exchanged zeolites were found to possess high catalytic activity in NH_3-SCO process. High N_2 selectivity, especially in the high temperature range, could be considered in the term of protection of NH_4^+ ions against oxidation and therefore their availability for reduction of NO_x (NH_3-SCR) [33]. Additionally, in contrast to non-porous materials [34], higher selectivity to N_2 has been reported for mesoporous materials with higher specific surface area providing larger number of acid sites accessible for reactants. The fabricated mesopores system facilitated the transport of the reactant molecules thus enhanced ammonia chemisorption and further transformation. A significant increase of additional centers for ammonia chemisorption was reported after deposition of transition metal oxides [34]. Indeed in the case of both hierarchical materials, i.e., Fe-M and Fe-D zeolites the enhanced external surface privileged the existence of isolated Fe-species.

3.4.3. NO sorption on vacuum treated catalysts

Sorption of small amounts of NO in studied zeolites produced a sharp band at ca. 1880 cm^{-1} of the Fe(II) mononitrosyl complexes $[Fe(NO)]^{2+}$ (Fig. 6, spectra a). With the respect to the band of gaseous nitrogen monoxide (1875 cm^{-1}) the negligible $[Fe(NO)]^{2+}$ band downshift indicated the minor weakening of the N—O bond in $[Fe(NO)]^{2+}$ adducts via π back donation effect. With time, the band at 1880 cm^{-1} decreases in intensity, while new bands at 2140 and 1640 cm^{-1} started to develop (Fig. 6, spectra b and c). The band at 2140 cm^{-1} was assigned to NO^+ species [35], which were easily produced after NO_x adsorption on various zeolites with the participation of the zeolite acidic Si(OH)Al groups [36] or formed via direct oxidation of NO by Fe^{3+} species [37]. One of the proposed schemes of the NO^+ formation includes the replacement of proton from the zeolite acidic hydroxyls by the NO^+ and the simultaneous formation of water molecule [38]. The IR bands at frequencies region 1650–1550 cm^{-1} are assigned to different NO_x^- species. Undoubtedly, the 1620–1640 cm^{-1} bands are characteristic for bridging nitrate species (NO_3^-) such as monodentate, bidentate, and bridging nitrates [35]. The formation of nitrate and nitro species is

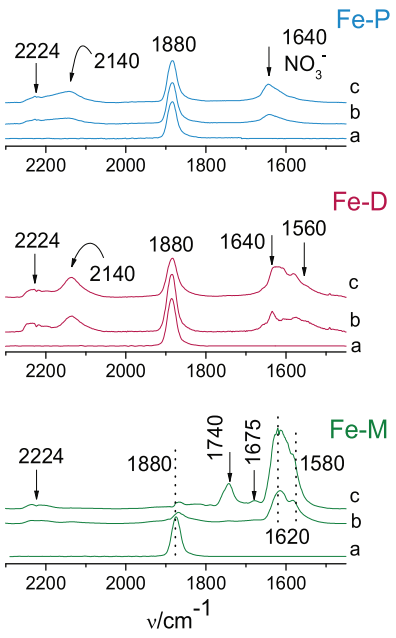

Fig. 6. FTIR spectra (nitrosyl stretching region) of Fe-zeolites collected at RT after adsorption of NO (a) and after 10 min. (b) and 30 min. (c) contact time.

accompanied by evolution of water because NO_x^- anions replace the surface OH groups. Thus, the H_2O contribution in the 1640 cm^{-1} band cannot be excluded. Similarly to the NO^+ formation, the evolution of NO_x^- moieties is accompanied by water formation. In this case, NO_x^- anions replace the surface OH groups [38]. Development of nitrates is concurrent with the N_2O appearance (2224 cm^{-1}). Described above catalytic behavior was reported for zeolite hosted various transition metal ions. Also for studied parent and hierarchical ZSM-5 this scheme was confirmed. Additionally, for Fe-M zeolite the generation of both NO_2 (the 1675 cm^{-1} band) and N_2O_4 (the 1740 cm^{-1} band) formed by NO_2 dimerization, was identified.

3.4.4. NO sorption on the catalysts with preadsorbed ammonia

Sorption of NO was carried out also for zeolites with preadsorbed ammonia molecules (Fig. 7). Interaction of ammonia with the acidic Si(OH)Al hydroxyls was manifested by development of NH_4^+ band at 1465 cm^{-1}, while ammonia coordinated to Lewis (NH_3-L) acid sites gave the band at 1610 cm^{-1} (spectrum a). Co-adsorption of NO at 100 °C on microporous zeolite Fe-P resulted in the appearance of only gaseous NO; the bands of NH_4^+ and NH_3-L remained unperturbed (Fe-P, spectrum b). After 5 min. contact time at 200 °C the IR cell was cooled down to room temperature and IR spectrum was collected (spectrum c). With the parallel reduction of the NH_4^+ band the nitrates (1620–1600 cm^{-1}), water (1635 cm^{-1}), and dinitrogen tetraoxide (1745 cm^{-1}), easily obtained by dimerization of NO_2, were distinguished among NH_3-SCR reaction products. Additionally, the bands both unreacted ammonia (detected in the N—H stretching region-spectra not shown) and NO in the gas phase (1875 cm^{-1}) were identified. The progress in NO reduction with ammonia was evidenced for zeolite Fe-D. When NO was contacted at 100 °C (Fe-D, spectrum b) and 200 °C (Fe-D, spectrum c) with Fe-D accommodating preadsorbed $[Fe(NO)]^{2+}$ mononitrosyl, nitrate (1620 cm^{-1}) and N_2O (2224 cm^{-1}) bands appeared with the simultaneous consumption of both NH_3-L adducts (1610 cm^{-1}) and ammonium ions (1465 cm^{-1}). Apart from unreacted NO, both in gas phase and in the form of monositrosyls, the presence of significant amounts of N_2O and nitrate species was evidenced. In this case all available ammonia molecules were

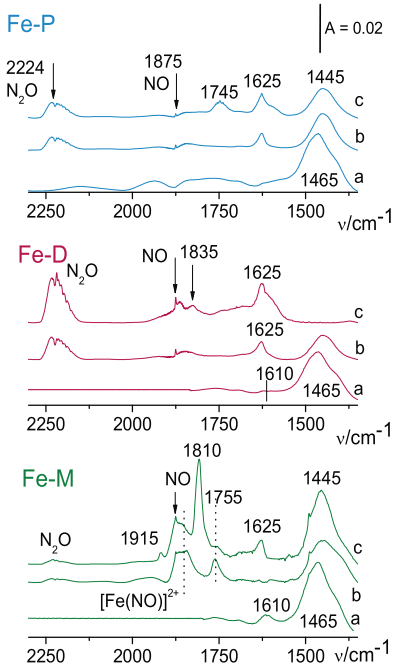

Fig. 7. (a) IR spectra of ammonia preadsorbed on Fe-exchanged zeolites. Spectra were collected upon saturation of the catalysts with ammonia at 100 °C and followed by the evacuation at the same temperature. (b) IR spectra collected at 100 °C after contacting of NO with Fe-zeolites with preadsorbed NH_3. (c) IR spectra collected at RT after 5 min. contact time at 200 °C of NO with Fe-zeolites with preadsorbed NH_3.

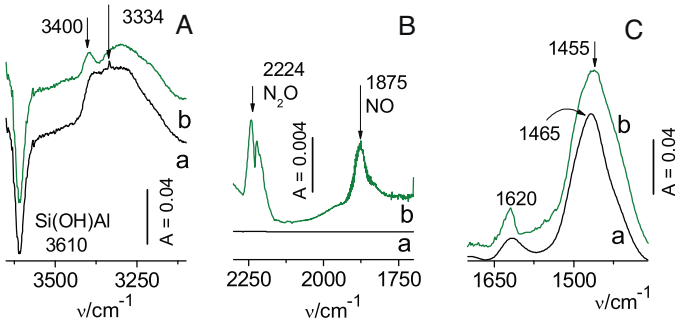

Fig. 9. IR spectra in N—H stretching (A), N—O stretching (B) and N—H deformation (C) region collected at room temperature for Fe-M zeolite preadsorbed with NH_3 (spectrum a), next heated to 350 °C (for 5 min.) and cooled down to room temperature (spectrum b).

consumed as no band at 1460–1440 cm^{-1} was detected (Fe-D, spectrum c).

The performance of Fe-M toward NH_3-SCR reaction differs from previously studied zeolites. At 100 °C the interaction of NO with Fe-M accommodating preadsorbed ammonia (Fe-M, spectrum b) resulted in development of $[Fe(NO)]^{2+}$ mononitrosyls (the band at 1850 cm^{-1}), N_2O (2224 cm^{-1}) and N_2O_4 (1755 cm^{-1}). At the same time, the band of NH_3-L vanished (1610 cm^{-1}), when the NH_4^+ (1465 cm^{-1}) was only slightly reduced. Therefore, it is believed that ammonia coordinatively bonded to Fe species was consumed in the NH_3-SCR reaction in the first order. In the spectrum collected at room temperature, corresponding to the reaction progress at 200 °C, both mononitrosyl $[Fe(NO)]^{2+}$ (1850 cm^{-1}) and dinitrosyls $[Fe(NO)_2]^{2+}$ complexes (the bands at 1915 and 1810 cm^{-1}, respectively) were identified (Fe-M, spectrum c). Among other products of the reduction of nitrogen monoxide by ammonia the NO_3^- nitrato species (1445 cm^{-1}), N_2O (2224 cm^{-1}), and H_2O (1630 cm^{-1}) were detected. It should be noted that all ammonium ions were consumed in the reaction. In the place of them the NO_3^- nitrato species were accommodated. Interestingly, only negligible amounts of N_2O were detected.

3.4.5. NH_3 and O_2 sorption on the studied catalysts

Fig. 8 depicts the spectrum of ammonia sorbed at 100 °C in studied Fe-zeolites (spectra a). The 1460 cm^{-1} band of ammonium ions (NH_4^+) was the most characteristic moiety attributed to the reaction of ammonia with strongly acidic Si(OH)Al groups (spectra a). The presence of a certain amount of ammonia coordinated to Lewis centers (electron-acceptor aluminum species of both Al-extraframework and Fe-species origin) was evidenced by the 1610 cm^{-1} band of a small intensity. Heating of the catalysts preadsorbed with ammonia in oxygen atmosphere up to 350 °C (spectrum b) for 5 min. resulted in ammonia oxidation. The products of NH_3-SCO reaction can be recognized in IR spectrum collected after IR cell cooling down to room temperature. Such procedure guaranteed the detection of all adsorbed species formed by ammonia oxidation. An appearance of new bands in the 1700–1350 cm^{-1} frequency region together with a decrease in intensity of the NH_3-L and NH_4^+ bands was noticed. The main oxidation products, i.e., H_2O and the NO_3^- nitrato species are characterized by the 1625 and 1455 cm^{-1} bands, respectively. NO and N_2O were not detected. Among studied zeolites, Fe-M revealed the highest intensieties of the oxidation product bands (mainly H_2O band), thus the highest catalitic activity.

Additional experiments of NH_3 transformation at 350 °C on the Fe-M surface monitored by FTIR spectroscopy (Fig. 9) showed that, in the oxygen absence, NH_3 previously deposited on the catalyst surface in the form of NH_4^+ ions (3400 and 1465 cm^{-1} bands) and NH_3-L moieties (1610 cm^{-1}) and even present in the gas phase (a sharp band at 3334 cm^{-1}) is finally transformed to H_2O (1620 cm^{-1}) and NO_3^- entieties (1440 cm^{-1}). However, in this case the NO, NO_2 and N_2O formation was significantly more pronunced than the NO_3^- nitrato species. This behavior proves the presence of high activity oxygen atoms that were attributed, in line with IR and UV–vis studies, to Fe(III)-oxo entieties, which in the absence of oxygen were enabled to oxidizie NH_3 to NO_x species. The mechanism of selective ammonia oxidation into nitrogen and water vapor is still

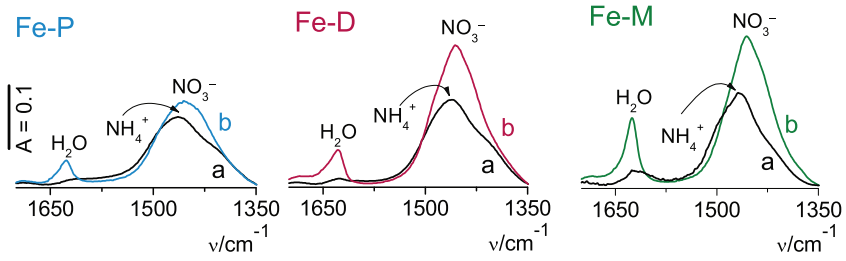

Fig. 8. Transformation of NH_3/O_2 mixture on zeolites Fe-P (A), Fe-D (B) and Fe-M (C).
a – IR spectra recorded after saturation of zeolites with NH_3 at 100 °C, b – IR spectra recorded at room temperature after heating of the catalysts pre-adsorbed with ammonia in oxygen atmosphere up to 350 °C for 5 min.

uncertain. However, high ability of Fe(III)-oxo species toward nitrogen oxides may suggest that that NH_3-SCO proceeds via the *i-SCR* mechanism. According to *i-SCR* mechanism, in the first step, ammonia is partially oxidized to nitrogen oxide which, in the next reaction step, is reduced to N_2 and/or N_2O by ammonia unreacted. However to justified such assumption the elementary surface reaction steps need to be identified.

4. Discussion

The Fe(III) ions introduction during ion-exchange is of a complex nature. The formation of mono-, di- or even polynuclear entities in the extraframework positions originates from hydrolysis supported by easy Fe(III) cation reducibility. The speciation of Fe moieties is hardly predictable being dependent not only on the Si/Al and Fe/Al ratios but also on Al atoms distribution in the zeolitic framework [39]. It has been reported that the isolated Fe^{2+} exchangeable cations are produced in ZSM-5 only in presence of Al pairs located in 6MRs, while Fe(III) hydroxocomplexes might be involved in interaction either with single Al atoms or Al pairs [39]. Dinuclear $[Fe–\mu O_2–Fe]^{2+}$ and $[Fe–O–Fe]^{2+}$ complexes might be also formed inside the zeolite channels and their charge is balanced by Al pairs. Although isolated Fe ions and Fe-oxo species of low nuclearity in the extraframework positions [40–42] were recognized as the most active sites for the NH_3-SCR process the structure ion-exchanged Fe-oxo species still remains unclarified.

In studied zeolites ZSM-5 of various pore topology a high population of an Fe(III)-oxo species confirmed by UV–vis and IR studies resulted from hydrolysis followed by the olation and oxolation processes that are induced by low aluminum content typical of studied ZSM-5 zeolites. Prevailing low concentration of AlO_4^- tetrahedra a noticeable population of highly dispersed mononuclear Fe(III)-oxo species is expected together with Fe(III)-oxo species, which positive charge is partially compensated by the zeolite framework. Among studied zeolites, the highest population of tetrahedral Fe(III)-oxo species was evidenced for mesoporous zeolite Fe-M synthesized via a direct synthesis route using the amphiphilic organosilanes. In Fe-D zeolite with the mesopore system fabricated by alkaline leaching the concentration of Fe(III)-oxo species was reduced in favor of oligomeric Fe(III)/Fe(II) oxide species. Indeed, the IR studies revealed the presence of Fe(III)-OH sites in studied mesostructured Fe-zeolites. Iron introduced to purely microporous zeolite (Fe-P) bears mainly oligomeric iron oxide clusters and Fe_2O_3 species. The uniform micro/mesoporous structure of Fe-M appears to prevent clustering of iron and preserves the Fe(III) species isolated inside the zeolite channels. In contrast to zeolite Fe-P, the catalysts based on zeolites with the hierarchical porous structure effectively activate the NH_3-SCR process in the low-temperature range, thus the mononuclear Fe(III)-oxo species are believed to facilitate highly active oxygen species being the most active moieties in this process. It should be underlined that among a variety of Fe species that could be offered also isolated Fe^{2+} cations were detected with CO as probe molecule in studied ZSM-5 zeolites [16,43].

Nevertheless, Fe^{2+} cations, occupying the exchange positions, were reported to be more inert for oxidation by molecular oxygen [39]. Indeed, pre-reduced zeolites accommodated mainly exchangeable Fe^{2+} cations presented lower activity than the non-reduced catalysts. Their activity considerably increased only at higher temperatures evidencing their low oxidation potential in the presence of oxygen-containing atmosphere. It points to the redox Fe(III)/Fe(II) cycle reversibility as the ruling factor in the oxygen atmosphere in the NH_3-SCR process. Regarding a lower activity of Fe^{2+} cations toward oxygen, the Fe(III)-oxo complexes were considered as the possible active sites. Moreover, an important role of acidic centers in chemisorption and activation of ammonia molecules in the NH_3-SCR process cannot be neglected [19].

The catalytic performance of mesostructured zeolites Fe-M and Fe-D in the NH_3-SCR process was characterized by a very high selectivity to N_2 in the temperature range up 375 °C. When the reaction temperature was increased above 375 °C a dramatic reduction in efficiency of the NO conversion related to side-process of direct ammonia oxidation by oxygen present in the reaction mixture was observed. The purely microporous zeolite Fe-P was found to be active above 400 °C, however, did not presented any drop of selectivity to N_2 in the entire temperature range. In line, such system revealed also lower activity in ammonia oxidation. The higher catalytic performances were found for both mesostructured Fe-zeolites.

The difference in catalytic activity of the studied zeolite ZSM-5 supports could be related to diverse nature of iron ions present in studied catalysts. It seems that high catalytic performance of the mesoporous catalysts in the NH_3-SCR and NH_3-SCO processes was related to the presence of iron species, mainly in the form of tetrahedral Fe(III), which was evidenced by DR UV–vis measurements. Judging for the high Si/Al ratio, mesostructured zeolites were able to accommodate high amounts of mono and dinuclear Fe(III)-oxo complexes [39] that guaranteed their high catalytic activity. Reduced concentration of Fe(III) oxo sites alongside with the presence of oligomeric iron oxide clusters and Fe_2O_3 species can be responsible for lower activity of purely microporous zeolite Fe-P. It should be noted that for the Fe-M and Fe-D catalysts enhanced Lewis acidity, originated from electron acceptor Fe sites, resulted in a similar catalytic activity in both reactions.

Lower catalytic performances in both NH_3-SCR and NH_3-SCO processes were presented by pre-reduced Fe-zeolites with negligible content of Fe(III) species [16]. It can be therefore assumed that Fe(III) species are the active sites providing a high selectivity to N_2 in the NH_3-SCO reaction.

The high selectivity to N_2 in the NH_3-SCO reaction is believed to originate also from strong Brønsted acidity of zeolites. An increase of Lewis acid centers for ammonia chemisorption after iron deposition should be considered as additional contribution into acidity picture [34]. Ammonia adsorption on both the Si(OH)Al groups and Lewis sites resulted in the NH_4^+ ions formation and NH_3-L adducts, resp., thus, the NH_3 concentration in gas phase decreased. Consequently, the formation of NO is also reduced since NO is generated mainly by the oxidation of gaseous NH_3. Therefore, the N_2 selectivity in the SCO reaction is improved.

The nature of iron species, that are active in the respective reaction pathways still requires comprehensive analysis in spite of broad spectrum of the studies over Fe-ZSM-5 in both the NH_3-SCR and NH_3-SCO processes [3,4,15,44]. The mechanism of NO reduction by NH_3 on Fe-ZSM-5 were widely studied and different reaction pathways were proposed [e.g.,15,44]. E.g., Long and Yang [44,45] suggested the reaction mechanism over Fe-ZSM-5 prepared by ion-exchange with $FeCl_2$. It was shown that oxidation of NO to NO_2 by O_2 on Fe^{3+} sites was the initial step of the NH_3-SCR reaction. In our case, NO adsorption experiment was performed in the absence of oxygen, therefore no significant NO oxidation to NO_2 should occur. Interaction of NO with tetrahedral Fe(III)-oxo complexes, may explain the NO_2 formation over Fe-M mesostructured zeolite, as it was suggested by Delahay et al. [15]. The formation of NO^+ over other catalysts was described above and was attributed to the direct oxidation of NO by Fe(III)-oxo species. The *i-SCR* mechanism was proposed for the process of selective catalytic oxidation of ammonia performed in the presence of Fe-ZSM-5 zeolites [3,4]. This mechanism was formulated based on catalytic tests of NH_3-SCR and NH_3-SCO together with FT-IR studies. Also in this case authors related the high catalytic activity in NH_3-SCO to simultaneous existence of Fe^{3+} and Fe^{2+} and suggested that the process proceeds with the formation of NO, as an intermediate. The IR spectra of the reaction between NH_3 and O_2 did not revealed the NO_x formation, what

was attributed to the high reaction rate between NH_3 and NO_x in the low-temperature range. This mechanism was proposed for Fe-ZSM-5 prepared by impregnation using $FeCl_2$, however, it seems that it could be valid also in the case of the studied samples.

Additionally, in line with literature reports [46,47], the presence of mesopores can enable faster transport of the reactants to active surface sites and reaction products in a reverse direction.

5. Conclusions

Mesoporosity in conventional ZSM-5 was created using amphiphilic organosilanes as a mesopore-directing agents and alkaline leaching with NaOH and TBAOH mixture. Development of mesoporosity did not affect purely microporous character of hierarchical materials. Implementation of Fe species to mesoporous ZSM-5 zeolites did not influence their textural parameters. Small decrease in micropore volume evidenced the partial plaguing of the micropore system due to accommodation of Fe-species. The DR UV–vis studies demonstrated that iron introduced to the mesoporous ZSM-5 materials was dispersed mainly in the form of isolated pseudotetrahedral Fe(III)-oxo sites. Oligonuclear Fe(III)/(II)-oxo clusters were detected in negligible amounts. Such properties resulted in high catalytic performances of hierarchical zeolites both in the NH_3-SCR and NH_3-SCO processes.

Acknowledgment

This work was financed by Grant No. 2013/09/B/ST5/00066 from the National Science Centre, Poland.

Appendix A. Supplementary data

Supplementary data associated with this article can be found, in the online version, at http://dx.doi.org/10.1016/j.apcatb.2015.05.053

References

[1] P. Forzatti, Appl. Catal. A 222 (2001) 221–236.
[2] G. Busca, L. Lietti, G. Ramis, F. Berti, Appl. Catal. B 18 (1998) 1–36.
[3] G. Qi, R.T. Yang, Appl. Catal. A 287 (2005) 25–33.
[4] G. Qi, J.E. Gatt, R.T. Yang, J. Catal. 226 (2004) 120–128.
[5] L. Chmielarz, M. Jabłońska, A. Strumiński, Z. Piwowarska, A. Węgrzyn, S. Witkowski, M. Michalik, Appl. Catal. B 130–131 (2013) 152–162.
[6] G. Olofsson, A. Hinz, A. Anderson, Chem. Eng. Sci. 59 (2004) 4113–4123.
[7] R.Q. Long, R.T. Yang, Chem. Commun. 17 (2000) 1651–1652.
[8] A. Akah, C. Cundy, A. Garforth, Appl. Catal. B: Environ. 59 (2005) 221–226.
[9] R.Q. Long, R.T. Yang, J. Catal. 201 (2001) 145–152.
[10] P. Boroń, L. Chmielarz, J. Gurgul, K. Łątka, B. Gil, J.-M. Krafft, S. Dzwigaj, Catal. Today 235 (2014) 210–225.
[11] P. Boroń, L. Chmielarz, J. Gurgul, K. Łątka, B. Gil, B. Marszałek, S. Dzwigaj, Micropor. Mesopor. Mater. 203 (2015) 73–85.
[12] A.L. Kustov, T.W. Hansen, M. Kustova, C.H. Christensen, Appl. Catal. B 76 (2007) 311–319.
[13] L. Kustov, K. Egeblad, M. Kustova, T.W. Hansen, C.H. Christensen, Top. Catal. 45 (2007) 159–163.
[14] M.H.S. Cho, R. Srivastava, C. Venkatesan, D.H. Choi, R. Ryoo, Nat. Mater. 5 (2006) 718–723.
[15] G. Delahay, D. Valade, A. Guzmán-Vargas, B. Coq, Appl. Catal. B 55 (2005) 149–155.
[16] K. Góra-Marek, K. Brylewska, K.A. Tarach, M. Choi, Dalton Trans. 44 (2015) 8031–8040.
[17] P. Sazama, B. Wichterlová, Š. Sklenák, V.I. Parvulescu, N. Candu, G. Sádovská, J. Dědeček, P. Klein, V. Pashkova, P. Šťastný, J. Catal. 312 (2014) 123–138.
[18] J. Pérez-Ramiréz, J.C. Groen, A. Brückner, M.S. Kumar, U. Bentrup, M.N. Bebbagh, L.A. Villaescusa, J. Catal. 232 (2005) 318–334.
[19] G. Delahay, M. Mauvezin, A. Guzman-Vargas, B. Coq, Catal. Commun. 3 (2002) 385–389.
[20] S. Bordiga, R. Buzzoni, F. Geobaldo, C. Lamberti, E. Giamello, A. Zecchina, G. Leofanti, G. Petrini, G. Tozzola, G. Vlaic, J. Catal. 158 (1996) 486–501.
[21] S. Brandenberger, O. Kröcher, M. Casapu, A. Tissler, R. Althoff, Appl. Catal. B 101 (2011) 649–659.
[22] X. Shi, H. He, L. Xie, Chin. J. Catal. 36 (2015) 649–656.
[23] M. Santhosh Kumar, M. Schwidder, W. Grünert, A. Brückner, J. Catal. 227 (2004) 384–397.
[24] H. Matsuura, N. Katada, M. Niwa, Micropor. Mesopor. Mater. 66 (2003) 283–296.
[25] G.D. Pirngruber, J.A.Z. Pieterse, J. Catal. 237 (2006) 237–247.
[26] K.A. Dubkov, E.V. Starokon, E.A. Paukshtis, A.M. Volodin, G.I. Panov, Kinet. Catal. 45 (2004) 202–208.
[27] G.I. Panov, E.V. Starokon, L.V. Pirutko, E.A. Paukshtis, V.N. Parmon, J. Catal. 254 (2008) 110–120.
[28] B.R. Wood, J.A. Reimer, A.T. Bell, M.T. Janicke, K.C. Ott, J. Catal. 225 (2004) 300–306.
[29] M. Mihaylov, E. Ivanova, N. Drenchev, K. Hadjiivanov, J. Phys. Chem. C 114 (2010) 1004–1014.
[30] T. Barzetti, E. Selli, D. Moscotti, L. Forni, J. Chem. Soc. Faraday Trans. 92 (1996) 1401–1407.
[31] K. Góra-Marek, M. Derewiński, J. Datka, P. Sarv, Catal. Today 101 (2005) 131–138.
[32] J. Datka, M. Kawałek, K. Góra-Marek, Appl. Catal. A: Gen. 243 (2003) 293–299.
[33] M. Jabłońska, A. Król, E. Kukulska-Zając, K. Tarach, L. Chmielarz, K. Góra-Marek, J. Catal. 316 (2014) 36–46.
[34] W. Yue, R. Zhang, N. Liu, B. Chen, Chin. Sci. Bull. 59 (2014) 3980–3986.
[35] K. Hadjiivanov, Catal. Rev. – Sci. Eng. 42 (2000) 71–144.
[36] F. Thibault-Starzyk, O. Marie, N. Malicki, A. Vos, R. Schoonheydt, P. Geerlings, C. Henriques, C. Pommier, P. Massiani, in: J. Čejka, N. Zilková, P. Nachtigall (eds.), Molecular Sieves: From Basic Research to Industrial Applications, Proceedings of the 3rd International Zeolite Symposium (3rd FEZA) Prague, Czech Republic 23–26 August 2005, Stud. Surf. Sci. Catal. 158 (2005) 663.
[37] K. Hadjiivanov, E. Ivanov, R. Kefirov, J. Janas, A. Plesniar, S. Dzwigaj, M. Che, Micropor. Mesopor. Mater. 131 (2010) 1–12.
[38] K. Hadjiivanov, J. Saussey, J.L. Freysz, J.-C. Lavalley, Catal. Lett. 52 (1998) 103–108.
[39] P. Sazama, B. Wichterlová, E. Tábor, P. Šťastný, N.K. Sathu, Z. Sobalík, J. Dědeček, Š. Sklenák, P. Klein, A. Vondrová, J. Catal. 312 (2014) 123–138.
[40] M. Iwasaki, K. Yamazaki, K. Banno, H. Shinjoh, J. Catal. 260 (2008) 205–216.
[41] S. Brandenberger, O. Krocher, A. Tissler, R. Althoff, Ind. Eng. Chem. Res. 50 (2011) 4308–4319.
[42] M.S. Kumar, M. Schwidder, W. Grünert, A. Brückner, J. Catal. 227 (2004) 384–397.
[43] M. Mihaylov, E. Ivanova, K. Chakarov, P. Novach, K. Hadjiivanov, Appl. Catal. A: Gen. 391 (2011) 3–10.
[44] R.Q. Long, R.T. Yang, J. Am. Chem. Soc. 121 (1999) 5595.
[45] R.Q. Long, R.T. Yang, J. Catal. 194 (2000) 80–90.
[46] L. Chmielarz, P. Kuśtrowski, R. Dziembaj, P. Cool, E.F. Vansant, Appl. Catal. B: Environ. 62 (2006) 369–380.
[47] L. Chmielarz, P. Kuśtrowski, M. Drozdek, R. Dziembaj, P. Cool, E.F. Vansant, Catal. Today 114 (2006) 319–325.